CHAPTER 4

Comparison of robot assisted incremental sheet forming (RAISF) and robot assisted incremental sheet hydroforming (RAISHF) of aluminium alloy 6061

4.1 Introduction

Once the setup had been developed fully and FEA and numerical modelling was done, a series of experiments were conducted. In this chapter, two types of experiments have been conducted: namely, fabrication of conical frustum using RAISF and RAISF. Although, several studies have been carried out on incremental sheet forming and hydro mechanical deep drawing related to wall angle but very limited work has been done on characterization of several other important aspects of ISHF. The theme of this chapter is to broadly compare the processes of RAISF and RAISHF, using 6 axis industrial robot. In the present work, RAISF and RAISHF processes have been used to form cones from sheets of aluminium alloy 6061. Formability of the undeformed sheets has been determined by Erichsen cup test. Straight groove test has been conducted on the samples made by RAISHF, after that regression analysis has been done to optimize the input parameters, such as tool speed, tool diameter and step depth, as mentioned in Section 2.4 of Chapter 2. Then, experiments have been conducted with the optimized parameters by the both, RAISF as well as RAISHF. The respective outputs of both the processes have been compared in terms of thickness distribution, microhardness, surface finish, strength, and major & minor strain in the plane of deformed sheet, and microstructures. Finally, LDH test has been conducted to compare RAISHF with the conventional biaxial stretching, fabricating hemispherical cups by the two processes.

4.2 Experiments with optimized parameters

Once the optimum parameters had been chosen as tool speed of 74.75 mm/sec, vertical step depth of 0.42 mm and tool diameter of 10 mm by regression analysis of results obtained from straight groove test, then all the experiments for further testing have been conducted using these parameters only. For robot assisted incremental sheet hydroforming (RAISHF), static pressure from back of the sheet was 1.5 bar. The pressure was taken from simulation analysis on ABAQUS. In case of ISHF, when the pressure was more than 1.5 bar, sheet under deformation got distorted and also got distorted during experimentation, so optimum pressure of 1.5 bar was chosen for incremental sheet hydroforming. Figure 4.1 gives an idea of the process of flow for RAISHF.

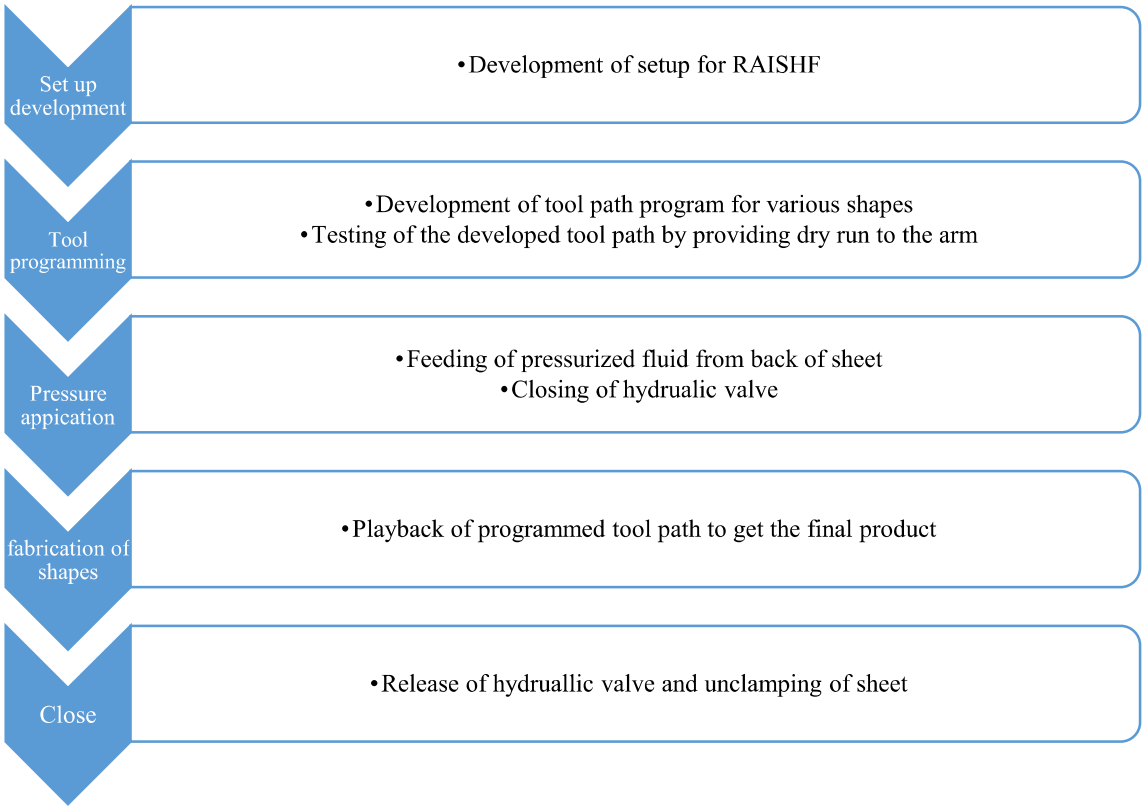

Figure 4.1: Flow diagram of RAISHF.

Various shapes were fabricated on the existing setup by both the processes; RAISF and RAISHF which are shown in Figure 4.2.

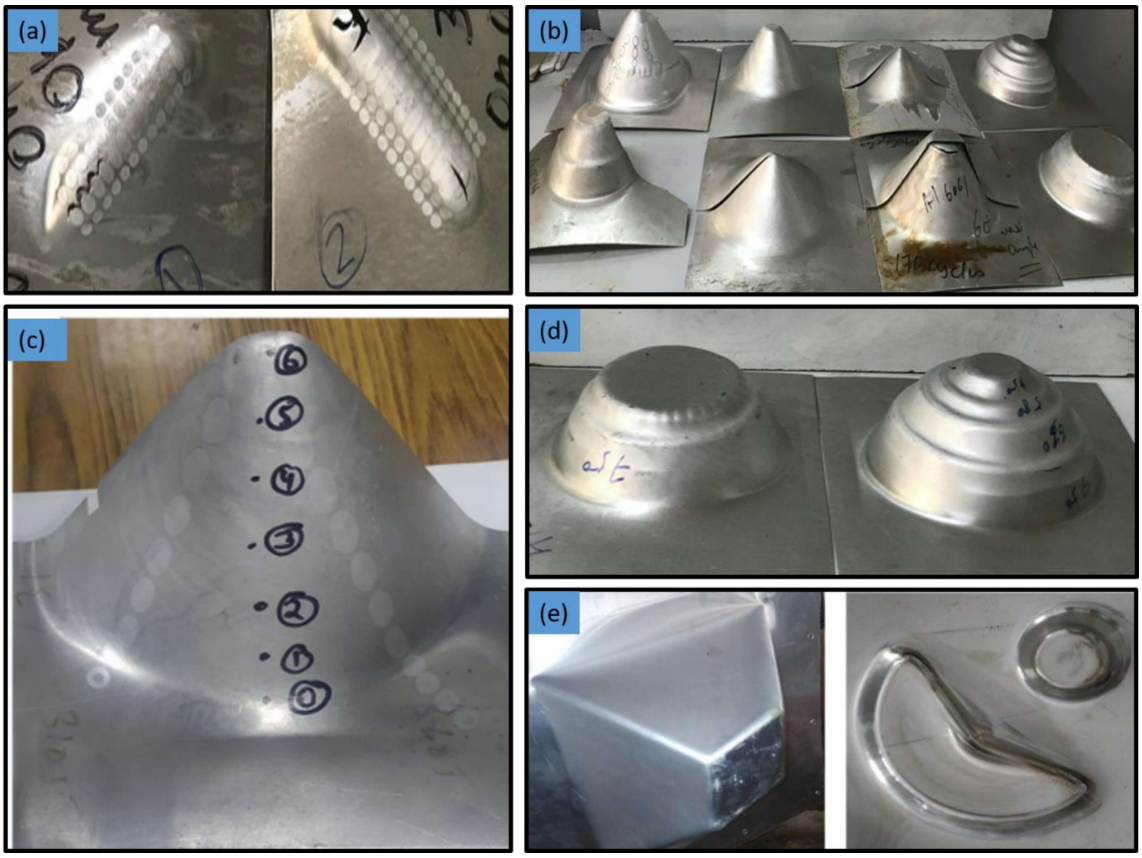

Figure 4.2: Various successfully made shapes on the existing machine of RAISHF: (a) straight groove, (b) conical shape, (c) multi-stage conical shape, (d) square pyramid, (e) multi-feature shape.

Once, different shapes had been fabricated successfully, several tests were conducted to compare the two processes. For the purpose of comparison and analysis, the conical shape with fixed wall angle has been considered.

4.3 Results and discussion

4.3.1 Maximum formable angle and spring back

In RAISF and RAISHF, the formability limit is decided by maximum wall angle which can be formed before fracture. To find out the maximum formable angle, a variable wall angle conical frustum (VWACF) has been made. The genetrix of VWACF is shown in Figure 4.3 (a). The samples made by RAISF and RAISHF are shown in Figure 4.3(b) and (c) respectively.

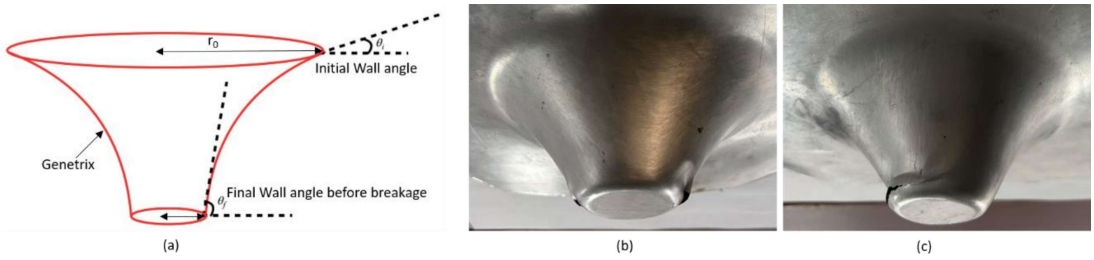

Figure 4.3: (a) Schematic diagram of VWACF with initial and final wall angle, (b) VWACF fabricated by RAISF, and (c) VWACF fabricated by RAISHF.

The details of the VWACF obtained by RAISF and RAISHF are given in Table 4.1.

Table 4.1: Details of VWACF fabricated by RAISF and RAISHF

Process	Initial Wall angle (Degrees)	Final Wall Angle (Degrees)	Theoretical depth of cone (mm)	Achieved depth of cone (mm)	Spring back (%)
RAISF	30	60	36.60	32.42	11.42
RAISHF	30	64	42.76	41.65	2.61

It can be seen from Table 4.1, that larger forming angle and smaller spring back can be achieved by RAISHF than that by RAISF. In case of RAISHF the forming angle and

forming depth increased by 6.67% and 28.47% respectively. Additionally, due to static fluid pressure from back, the spring back occurring during incremental forming was reduced appreciably. The spring back reduced by 77.14% in case of RAISHF with respect to that in RAISF.

4.3.2 Thickness distribution

The fixed angle conical frustum of maximum wall angle as obtained for VWACF has fabricated by RAISF and RAISHF with sheets of Aluminium alloy 6061, under the experimental condition, as optimized after straight groove testing. The initial radius of the cone circle has been taken as 100 mm. The maximum wall angles of the cones formed from sheet of the alloy 6061, by RAISF and RAISHF are found to be 60^0 and $64^{0,}$ respectively, the details of which are given in Table 4.2. These two cones have been used for comparison of mechanical properties of the cones formed by RAISF and RAISHF.

Table 4.2: Experimental details of forming conical shapes of maximum fixed wall angles.

Process	Fluid Pressure (bar)	Theoretical wall angle (^{0})	No. of cycles till onset of fracture	Depth achieved (mm)	Spring back (%)
RAISF	Nil	60	225	86.62	8.33
RAISHF	1.5	64	225	92.58	2.03

Once the cones have been fabricated successfully, their respective depths are measured using depth measuring blade of Vernier calliper of least count 0.01 mm. The formed cone was cut precisely into two halves with wire electro-discharge machining (W-EDM) and the conical region was divided into 7 sub-regions (0-6), as shown in Figure 4.4 (a). The

thickness in the different regions has been measured by micro meter with conical tips and least count of 0.001mm. Region-0 is the undeformed region where thickness is 1.05 mm. The thickness plots for the RAISF and RAISHF processes are shown in Figure 4.4(b). It was found that there was a certain amount of thinning of the sheet associated with the process of RAISF as well as RAISHF. As the cone is formed, the thickness of the sheet decreased. The sheet is found to be thinnest in the region 1-2 which is nearly at the start of the conical frustum. The sheet is found to be thinnest in this region because of combined bending and stretching taking place in this region. The thickness of the cone is found to be nearly uniform in the regions 2-5. In these regions, the thickness of the sheet can be approximated by sine law. This trend is in accordance with the findings of Ambrogio et al. [138] and Young and Jeswiet [139], who showed that in middle region of the formed cone, thickness prediction by sine law is most accurate. The blue line in Fig. 4.4(b) shows the thickness, as predicted by the sine law for spinning, $t = t_0 \sin\theta$ [19]. In region 6, which is near the undeformed cone, the thickness again increases. The average sheet thickness (t_{avg}) in the regions 1-5, in the 4 processes is given in Table 4.3. In case of RAISHF, the sheet undergoes thinning in the region 0-1, in region 2-5 the thickness of the sheet becomes uniform and then the thickness increases in region 6.

Table 4.3: Average thickness of sheet along the length of the cone wall

Process	Average value of sheet thickness (t_{avg}) (mm)	Minimum thickness (mm)
RAISF	0.736	0.752 mm
RAISHF	0.825	0.623 mm

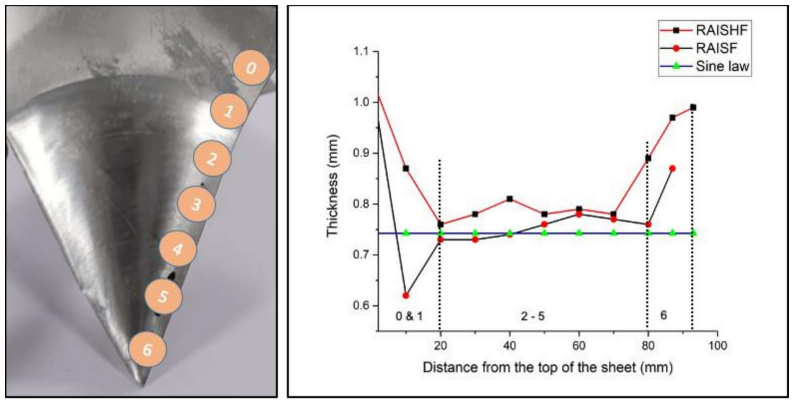

Figure 4.4: (a) Various regions along the length of the cone and (b) Variation of wall thickness of cones formed by ISF and ISHF processes, along the meridional plane.

It has been found that in RAISF, sheet thinning occurs and thickness in the middle region of 1-5, can be approximated by sine law due to shear nature of deformation in this region. However, for the RAISHF, thickness in the region 1-5 is more than that in RAISF, hence sheet thinning can be avoided to a significant extent. The average sheet thickness of the cone formed by RAISHF is found to be 12.09% more than that formed by RAISF. This can be due to relatively more uniform strain distribution as observed in hydroforming. It has been further observed that the range of deviation of thickness values from average value varied from -9.87% to 17.27% in case of RAISF whereas in case of RAISHF the variation lied in the range of -7% to 5%. This can be said with affirmity that thickness distribution and hence strain distribution is more uniform in case of RAISHF than in RAISF due to hydrostatic nature of fluid pressure from back.

4.3.3 Tensile test

In order to compare the tensile properties before and after forming, uniaxial tensile tests have been conducted on the samples prepared from annealed sheets and after forming cone,

on a 100 kN INSTRON (MODEL 8801). The samples have been prepared as per the standard ASTM/E8 [140]. After the formation of cone, tensile samples have been prepared along the length of the frustrum of the cone, along circumference, and at 45degree to length, as shown in Figures 4.5(a), 4.5(b) and 4.5(c) respectively. Since there can be some anisotropic effect in the formed product, hence the test samples have been prepared in three orientations: namely, (a) along the length of the formed cone (meridional direction) (b) along the direction of the tool motion (c) along 45. Tensile samples prepared from the various orientations are shown in Figure 4.5(d).

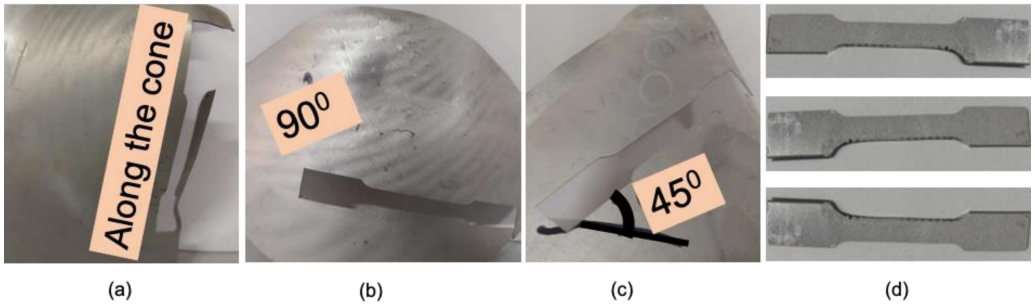

Figure 4.5: Tensile samples made from different orientations of the cone; (a) along the length of the cone (meridional direction), (b) along the direction of the tool motion (circumferential direction), (c) along 45^0 direction, and (d) Various tensile samples

The specimens mounted on the uniaxial tensile testing machine and those before and after test are shown in Fig 4.6.

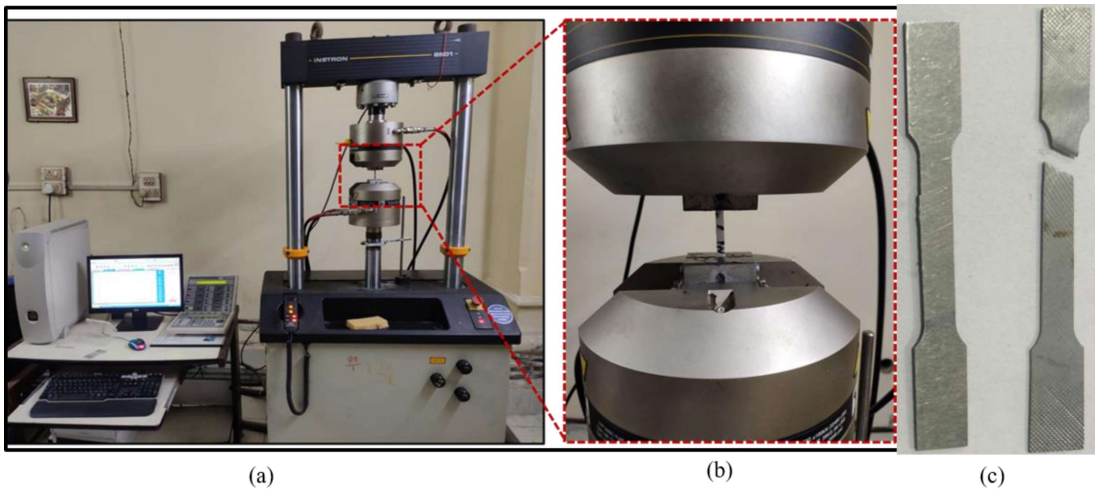

Figure 4.6: (a) UTM setup for tensile testing with mounted sample, (b) sample for tensile test marked on the cone for cutting, (c) fractured tensile tested samples.

The engineering stress strain curves for the various tests conducted are shown in Figure 4.7 and the tensile properties obtained in various directions are presented in Table 4.4.

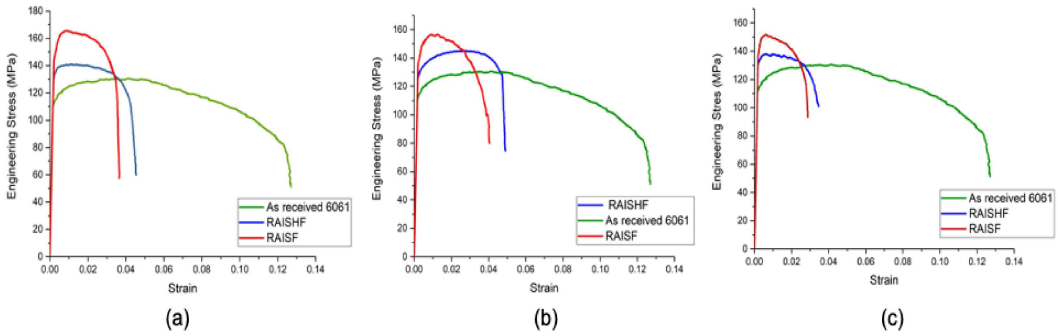

Figure 4.7: Tensile stress strain plots in different orientations of the formed cones: (a) along the tool direction (circumferential direction) (b) along the length of the cone (meridional direction) (c) at 45^0 from the longitudinal direction.

Table 4.4: Tensile properties of the cones formed by RAISF and RAISHF, in different orientations

Tensile properties along tool direction (circumferential direction)			
Parameters	Undeformed	RAISF	RAISHF
0.2% offset Yield Strength (MPa)	112	142	133
UTS (MPa)	127	162	136
Elongation (%)	12.16	3.81	4.14
Tensile properties along the length of cone			
0.2% offset Yield Strength (MPa)	112	130	123
UTS (MPa)	127	157	141
Elongation (%)	12.16	4.12	5.04
Tensile properties of the cone along 45 degrees			
0.2% offset yield strength (MPa)	112	145	126
UTS (MPa)	127	146	128
Elongation (%)	12.16	2.54	4.08

It can be seen from Table 4.4 that tensile properties in different directions are different, showing anisotropy in the formed cone. It is worthwhile to note that, the tensile test performed on the samples taken from formed cone has pre-strain due to which it showed less elongation during tensile test. The strength of the cone was maximum in the circumferential direction. Additionally, it can also be seen from the Table that strength of samples taken from the cone formed by RAISHF is relatively less. However, elongation is more in those samples. The reason for relatively lower strength in the case of the hydroformed cone can be stress delocalization due to the hydrostatic fluid pressure from the back. The pressure-induced ductility accounts for the rise in ductility of the cone formed by RAISHF.

4.3.4 Microhardness test

The hardness of the sheet, following RAISF and RAISHF, needs to be assessed because it is vital for the fabricated parts to be strong and hard. Microhardness test has been done to assess hardness of the formed cones. Average microhardness of undeformed 6061 sheet is found to be 62.5 VHN. After the cone had been successfully fabricated, samples have been taken from each region (0-6) and microhardness of the different regions has been measured. The applied load was 100gm and indentation time was 10 seconds. For each region, 4 micro measurements have been made at different points on the samples and average of the four values has been taken as microhardness of that region. Testing has been carried out on OMNITECH microhardness testing Machine. The respective values of microhardness of the cones of Al alloy 6061 formed by the RAISF and RAISHF are recorded in Table 4.5.

Table 4.5: Average microhardness values obtained in different regions of the formed cones.

Region	RAISF (VHN)	RAISHF (VHN)
0	75.0	75
1	81.6	74.8
2	90.5	70.5
3	19.2	81.2
4	104.2	80.2
5	93.5	98.2
6	83.2	76.0

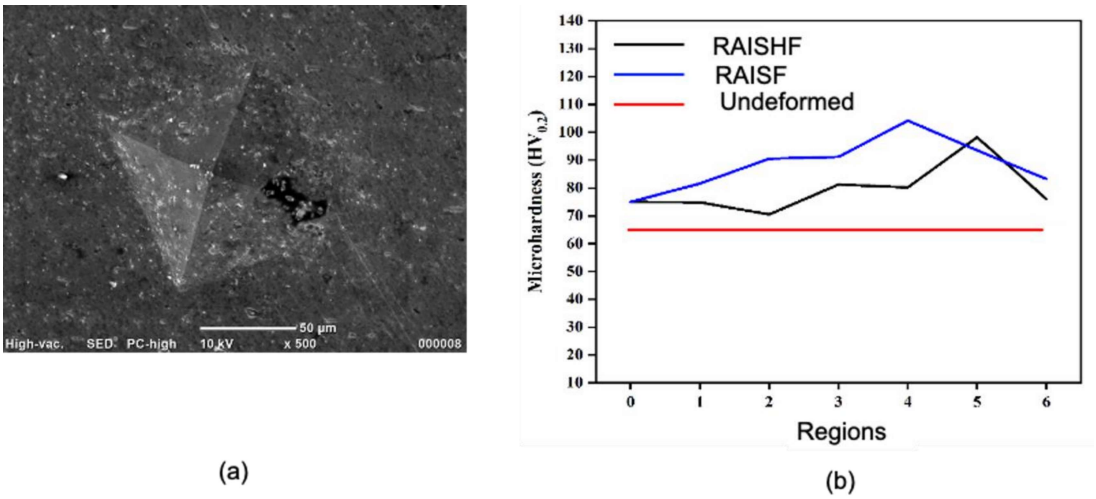

Figure 4.8(a) Indentation mark of microhardness measurement (b) comparison of microhardness of the cones formed by RAISF and RAISHF.

As can be seen from Table 5, microhardness values of the samples taken from the RAISF cone are higher in comparison with the samples taken from the respective regions of the cone formed by RAISHF. The microhardness of the samples taken from the formed cones is found to be higher than that of the undeformed sheet, due to strain hardening induced during the process of forming. It may be seen from Figure 4.8 that microhardness is maximum in middle region of the cone; it suggests that this region has undergone maximum strain hardening due to maximum straining as observed from the thickness distribution curve.

4.3.5 Surface finish

Measurements have been made to assess surface quality of the cones formed by RAISF and RAISHF processes. As surface finish is an important aspect to assess the quality of the

sheet metal formed products, the effect of the process on the surface finish has been investigated. Surface finish of the inner side of the cones has been measured and compared. Since this side remains in direct contact with the forming tool, the roughness of this is likely to be more than that of the outer surface. Samples have been taken from region 3 of the formed cones, as this is region of maximum straining. Surface roughness of the undeformed and deformed sheet has been measured by R_a value, moving the stylus knob over the sample. This test has been carried out on the Mitutoyo Surftest SV-2100 machine. The sampling length was 0.8 mm, the number of samplings was 5, and the travel length was 4.8 mm. Surface profiles of all the samples are shown in Fig. 4.9 (a), (c) and (e).

Fi

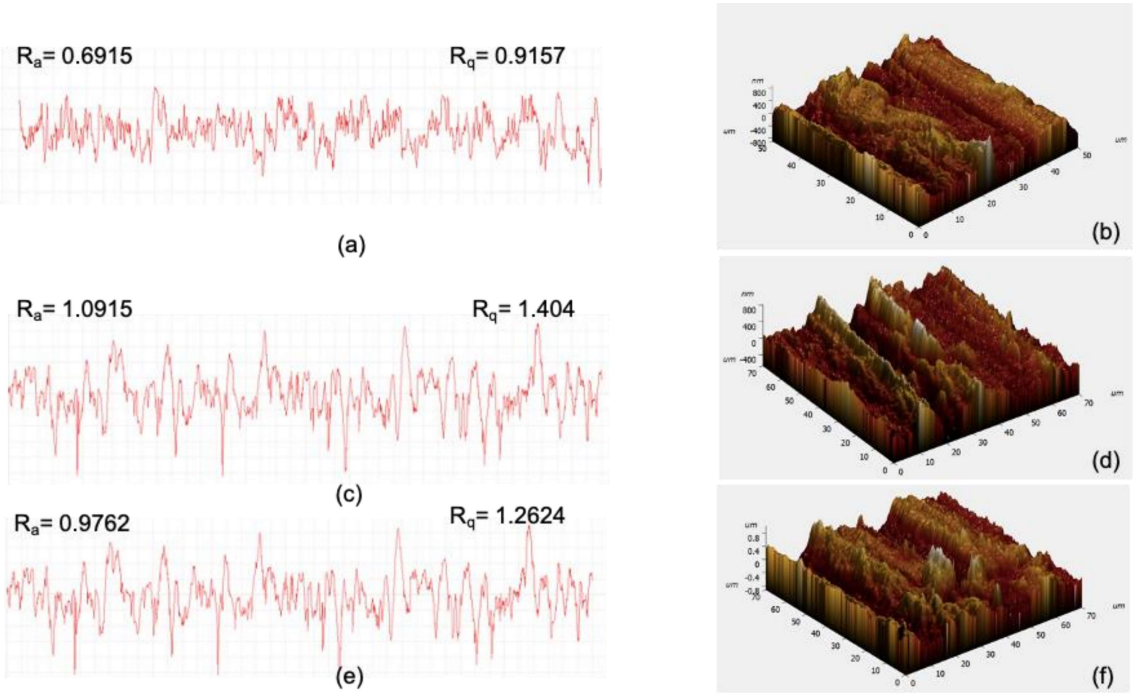

Figure 4.9: Different surface profiles: (a)surface roughness profile of undeformed AA6061 (b) AFM image of undeformed AA6061 (c) surface roughness profile of AA6061 formed by RAISF (d) AFM image of AA6061 formed by RAISF (e) surface roughness profile of AA6061 formed by RAISHF (f) AFM image of AA6061 formed by RAISHF

It has been found that surface finish is better in case of the hydroformed cone, in comparison with that of the conventional incrementally formed cone. R_a value from RAISF is found to be 1.0915μm whereas from RAISHF it is 0.9762 μm. Thus, there was improvement of 10.56% in surface finish of the cone formed by RAISHF. Further, atomic force microscopy (AFM) has been conducted on the samples to see surface topology of the undeformed and formed samples. The AFM micrographs are shown in Figure 4.9 (b), (d) and (f). It can be seen from the AFM images that surface topology of the hydroformed sample has more uniform in comparison with that of the incrementally formed samples. It can be concluded that using static fluid pressure from back side can improve the surface quality of the formed product.

4.3.6 Forming limit curve of RAISF and RAISHF

For comparison of strain in the plane of the formed sheet, cones of fixed wall angle of 60^0 fabricated by RAISF, and of 64^0 fabricated by RAISHF have been taken. The undeformed sheets have been engraved with circular grid pattern, and these became elliptical when fabricated into conical shapes. Both the cones have been engraved with circular grid patterns. The gridding method recommended by Keeler [140] has been used for engraving different regions of the sheet using a 50 W Fibre laser. Various grid patterns and methodology of grid marking has been discussed by Ozturk et al. [82]. The diameter of the engraved circular pattern is 10mm. After deformation, the circular pattern became elliptical, and the major and minor axes have been measured using a Vernier calliper of least count 0.01 mm. Once the major and minor axes have been measured, the true major strains and minor strains are calculated using equations (1) and (2)

$$\text{Minor strain} = \ln\left(\frac{Major\ Axis\ length - Circle\ diamter}{Circle\ diameter}\right) \quad (1)$$

$$\text{Minor strain} = \ln\left(\frac{Minor\ Axis\ length - Circle\ diamter}{Circle\ diameter}\right) \quad (2)$$

The scatter plot of major strain vs minor strain for RAISF and RAISHF is shown in Figure 4.10 which represents forming limit for the two processes

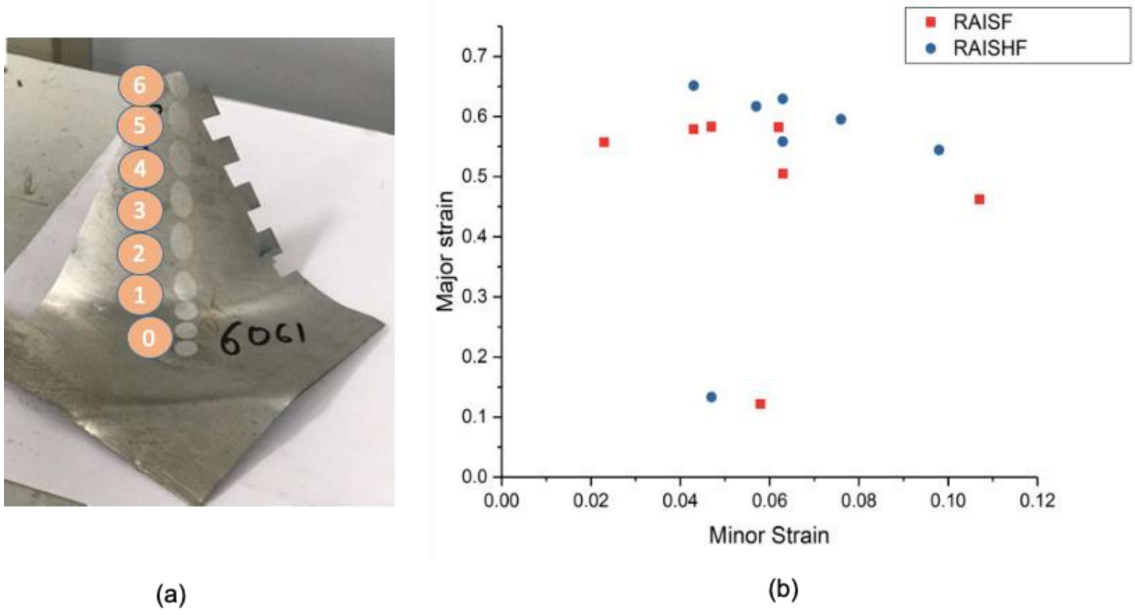

Figure 4.10: (a) Distorted grid patterns in different regions of the formed cone (b) comparison of forming limit curve of the cones formed by RAISF and RAISHF

It can be seen from Figure 4.10 (b) that more safe strain can be obtained in case of RAISHF than in RAISF. Because of fluid from the back side of sheet, the fluid pressure can create a hydrostatic condition which contributes towards pressure induced ductility to sheets [125, 141]. Hence, the sheet with fluid from back side can be more ductile and larger formability can be achieved by RAISHF than by RA.ISF.

4.3.7 Residual stresses

Once the cones got successfully fabricated, the residual stress of the samples taken from region 4 of the cone has been measured. Samples have been prepared and d-$\sin^2\Psi$

methodology has been adopted for calculation of residual stresses in the samples [142-144]. Three samples have been taken; (a) undeformed sample (b) Sample from cone made by RAISF (c) Sample from cone made by RAISHF. The characteristic diffraction pattern of the material, from the undeformed sheet has been taken and compared with the samples from the cones formed by RAISF and RAISHF processes. The definition of specimen frame of reference (FOR), rotated user FOR and different rotation and tilt angles are shown in Figure 4.11.

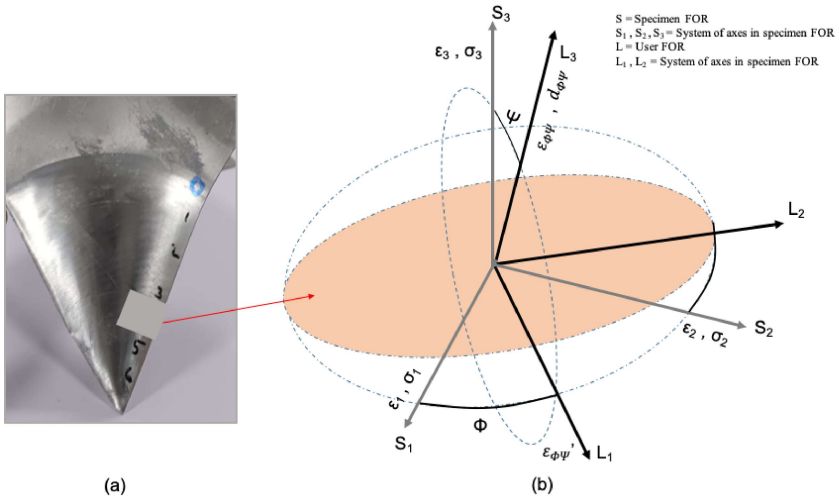

Figure 4.11: (a) Sample for XRD (b) Definition of different FORs and different angles for XRD examination.

S_i represents the specimen FOR where S_3 is perpendicular to specimen plane and S_1 and S_2 represent two perpendicular directions in the plane of the specimen. L_i is the user FOR with L_3 perpendicular to the (hkl) plane undergoing diffraction and L_1 and L_2 represent two perpendicular directions in (hkl) plane. In d-sin$^2\Psi$ approach, the strain is calculated by shift in the diffraction peak which gives the change in interplanar spacing. The strain component $\varepsilon_{\varphi\psi}$ can be written for the rotation angle (Φ) and tilt angle (Ψ) with interplanar spacing determined from the diffraction peak for a certain plane as

$$\varepsilon_{\varphi\psi} = \frac{d_{\varphi\psi} - d_0}{d_0} \quad (3)$$

Where $d_{\Phi\Psi}$ is the inter planar spacing at (Φ, Ψ) and d_0 is the interplanar spacing for strain free lattice spacing. In a standard stress measurement, $d_{\Phi\Psi}$ is varied and is measured as a function of Ψ. The expression for principal strain component can be finally written as

$$\varepsilon_{\varphi\psi} = \frac{d_{\Phi\Psi} - d_0}{d_0} = \frac{1+\mu}{E}(\sigma_{11}cos^2\varphi + \sigma_{12}\sin 2\varphi + \sigma_{22}sin^2\varphi - \sigma_{33})sin^2\psi + \frac{1+\mu}{E}\sigma_{33} - \frac{\mu}{E}(\sigma_{11} + \sigma_{22} + \sigma_{33}) + \frac{1+\mu}{E}(\sigma_{13}\cos\varphi + \sigma_{23}\sin\varphi)\sin 2\psi \quad (4)$$

For biaxial plane stress condition

$$\frac{d_{\Phi\Psi} - d_0}{d_0} = \frac{1+\mu}{E}(\sigma_{11}cos^2\varphi + \sigma_{22}sin^2\varphi)sin^2\psi - \frac{\mu}{E}(\sigma_{11} + \sigma_{22}) \quad (5)$$

$$d_{\Phi\Psi} = \frac{1+\mu}{E} d_0(\sigma_{11}cos^2\varphi + \sigma_{22}sin^2\varphi)sin^2\psi - \frac{\mu}{E} d_0(\sigma_{11} + \sigma_{22}) + d_0 \quad (6)$$

The X-ray diffraction can give the value of inter-planar spacing d_0 and $d_{\Phi\Psi}$. The plot between $d_{\Phi\Psi}$ and $\sin^2\psi$ is made by linear fit and measuring the slope and intercept can give the value of stress components. If there is presence of shear components then ψ – splitting occurs.

The nature of residual stress in both the samples, taken from the cones formed by RAISF and RAISHF is found to be tensile. Additionally, because of ψ – spilt it can be said that shear stress is also produced during both of the processes. The values of stresses for the undeformed, RAISF and RAISHF samples for $\Phi = 0^0$, 45^0 and 90^0 are given in Table 4.6.

Table 4.6: Values of residual stresses in different samples, at different orientations.

Name of sample	$\Phi = 0^0$	$\Phi = 45^0$	$\Phi = 90^0$
Undeformed	8.4 ± 0. 3 Mpa	43.8 ± 0.3 MPa	78.8 ± 0.3 MPa
RAISF	52.3 ± 1.1 Mpa	64.9 ± 1.1 MPa	77.5 ± 1.1 MPa
RAISHF	45.9 ± 0.4 Mpa	44.5 ± 0.4 MPa	43.0 ± 0.4 MPa

It can be seen from Table 4.6 that, the nature of residual stress is tensile in the cones formed by both the processes, and tensile residual stress is relatively larger in the cone formed by RAISF.

4.3.8 Microstructure evolution

The study of microstructure and texture evolution has been done by performing Electron Back Scattered Diffraction (EBSD) on Zeiss Gemini, equipped by OXFORD fast CCD detector. For analysis of data obtained from EBSD, the TSL-OIM software has been used. Three samples have been tested: (a) Undeformed sample taken from top of the cone (UD) (b) Sample taken from region 4 of cone formed by RAISF (c) Sample taken from region 4 of cone formed by RAISHF. EBSD data has been used for getting inverse pole Figure (IPF), image quality (IQ) maps, and grain average misorientation (GAM) plot. The IPF plot, IQ map and GAM plot of undeformed samples are given in Figure 4.12. The IPF plots are taken with a step size of 0.15μm.

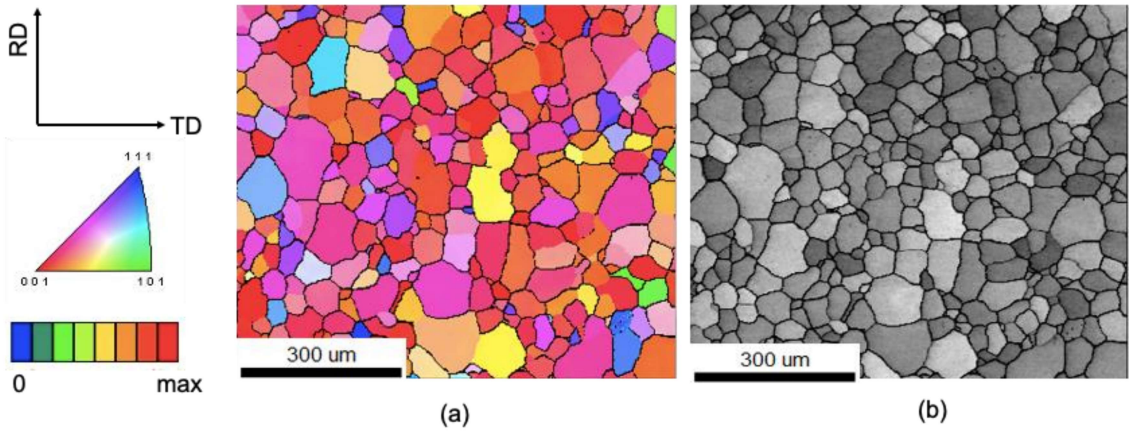

Figure 4.12: EBSD of undeformed AA6061 in annealed condition (a) IPF plot and (b) IQ map.

It may be observed from Figure 4.12(a) and 4.12 (b), that moderate to coarse equiaxed grains are present in the polycrystalline matrix as the sheet was in fully annealed condition. The average grain size is found to be 8.3 μm. The grains appear to be relaxed due to absence

of any strain as annealing caused recrystallization giving rise to stress free grains. Figure 4.13 gives the plot of number fraction vs. misorientation angle.

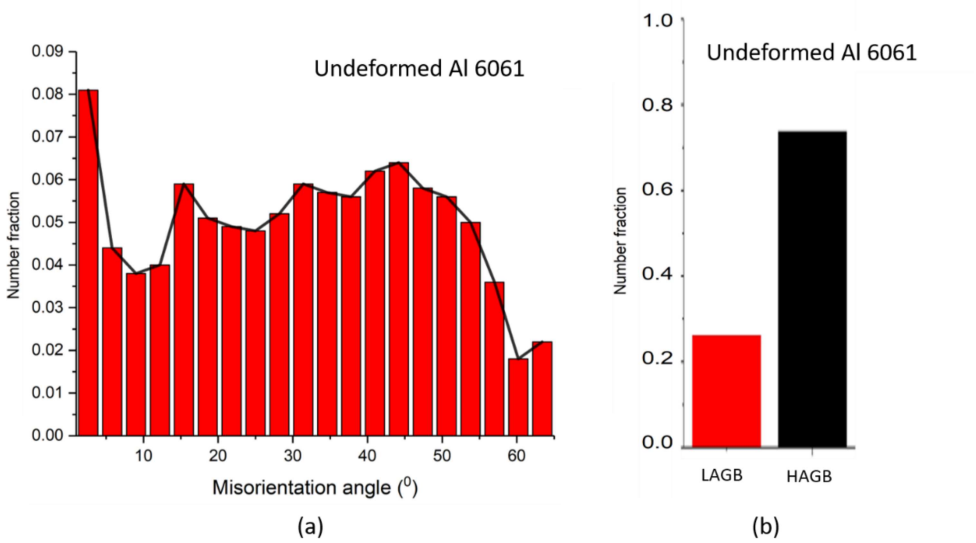

Figure 4.13: Distribution of misorientation angle in the undeformed 6061 sample.

The misorientation angle greater and less than 15º, are associated with high angle grain boundary (HAGB), and low angle grain boundary (LAGB) respectively. The misorientation angle analysis data shown in Figure 4.13(a) show that high density of high angle grain boundaries (HAGBs) is present in the undeformed sample. It has been further calculated that 26.2% of grains are separated by low angle boundaries and 73.8% of the grains are separated by high angle boundaries. As cone is formed, the sheet gets deformed, due to this deformation, the grains got elongated along the tool motion. The IPF of sample deformed by RAISF and RAISHF are shown in Figure 4.14.

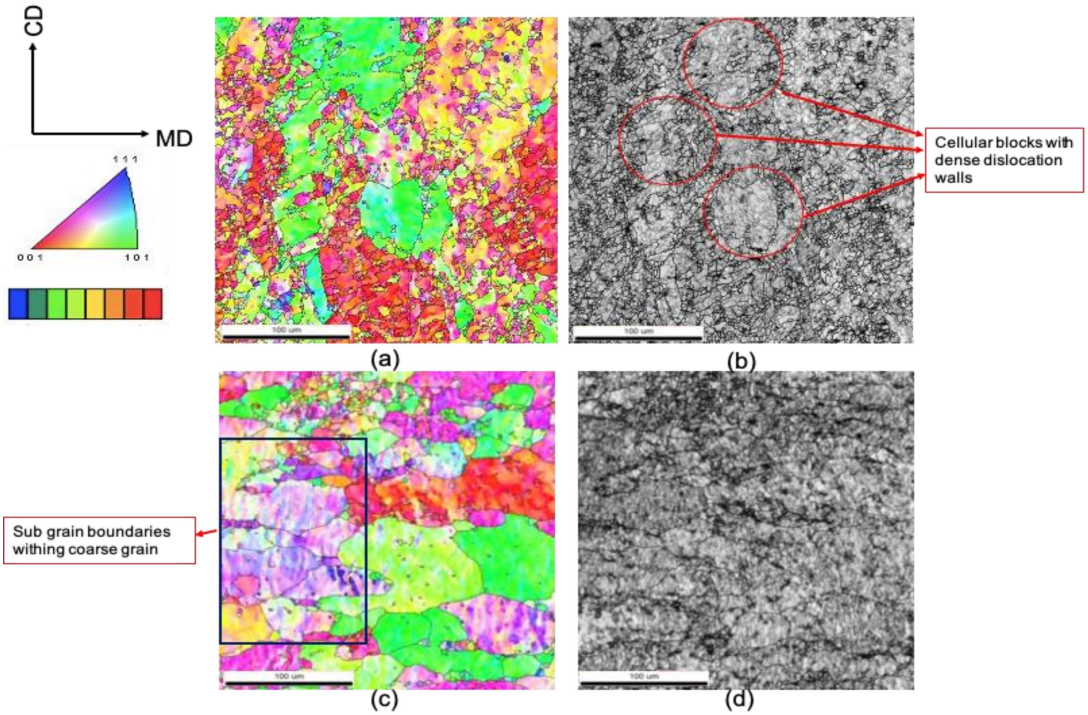

Figure 4.14: (a) IPF of sample formed by RAISF, (b) IQ map of sample formed by RAISF, (c) IPF of sample formed by RAISHF, and (d) IQ map of sample formed by RAISHF.

It has been observed that grains got refined due to cold work imparted to the sheet. The average size of grains in the samples obtained from the cones formed by RAISF and RAISHF, are found to be 5 μm and 7.1 μm respectively. Refined grains can be seen from the IQ maps with different colours for LAGBs and HAGBs shown in Figure 4.15 (a) and 4.15(c). Because severe plastic deformation occurred in both the processes, it caused grain fragmentation and led to fine grain evolution. It can be seen from IPF of RAISF sample, that there are cell blocks present with dense dislocation walls. The cell blocks form at the start of the deformation which activates different slip systems in a grain [145, 146]. It has been observed from IPF of the undeformed sample that there were LAGBs present in it. As the sheet gets deformed, these LAGBs act as a site for nucleation of new cell block and the formed cellular blocks are surrounded by dense dislocation walls. In case of RAISHF, it

has been observed that apart from cell blocks with dense dislocation walls, coarse grains are present which contained fine grains and sub grains with metasTable grain boundaries which can be observed by colour contours within the coarse grains.

Although, in case of both RAISF and RAISHF grain refinement occurred but in case of RAISF finer grains are found to be present. Presence of finer grains in RAISF sample can also be confirmed by the results of tensile test and Hall-Petch equation $\sigma_a = \sigma_a + \frac{K}{\sqrt{a}}$,where a is the grain size. More tensile residual stress observed in case of RAISF also confirm this result. According to Hall -Petch relation, sample with finer grains particles have higher strength. It has been observed from the tensile test that the strength of the RAISF sample is more than that of the RAISHF sample. Hence, grain size in case of RAISF sample should be less. A similar result for incremental sheet forming has been observed by Chang at al. [147] and Abhishek et al. [148] where finer grain particles were observed in the deformed sample. In case of RAISHF more strain has been obtained, the result being supported by Kernel misorientation map (KAM). The KAM plot of RAISF and RAISHF samples are given in Figure 4.15 (b) and 4.15 (d) respectively. It can be seen from KAM plot that RAISHF sample has undergone more strain due to larger formability achieved during the process.

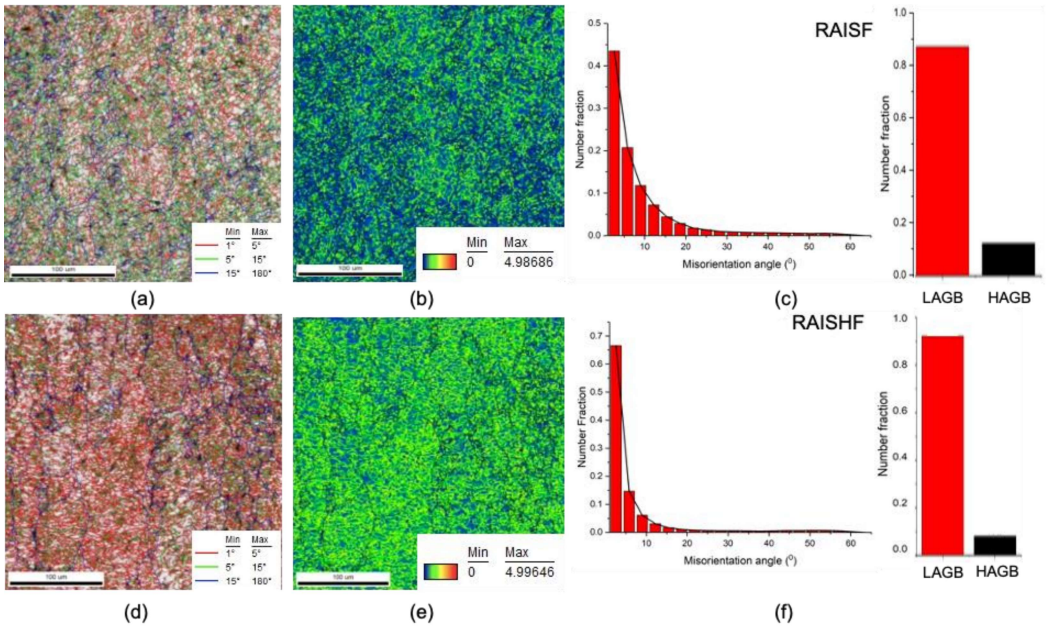

Figure 4.15: (a) Grain boundary map of RAISF sample, (b) KAM map of RAISF sample, (c) Distribution of misorientation angle in the RAISF sample, (d) Grain boundary map of RAISHF sample, (e) KAM map of RAISHF sample, and (f) Distribution of misorientation angle in the RAISHF sample.

Further, it can be observed from Figure 4.15 (a) and 4.15 (c) that high density low angle or sub-grain boundaries are present in both the samples. LAGBs are a characteristic of the processes involving cold work [149-151]. Further, in case of RAISF, majority of LAGBs lied in the region of $5^0 – 15^0$ whereas in case of RAISHF they are found to be in the region of $1^0 – 5^0$. It can be seen from the IPF of RAISHF sample that there are metasTable sub grain boundaries which can be due to dynamic recrystallization happening during RAISHF.

4.4 Limiting dome height test

From the tests performed in the previous sections, it is clear that RAISHF is a better process of sheet forming than RAISF in terms of mechanical properties of the fabricated component. It needs to be further checked that how does RAISHF perform with respect to the conventional forming operations. To compare the formability by RAISHF with

conventional forming operation, first LDH test has been done on double action hydraulic press with a main ram capacity of 100 kN and secondary ram capacity of 50 kN as shown in Fig. 4.16 (a). The hydraulic ram was equipped with force measuring device which measured the force applied by ram. Hemispherical dome of 100 mm diameter has been formed. While performing the LDH test, feed rate has been kept at 1mm/s. The diameter of the punch was 100mm. The limiting height before the onset of breakage was found to be 17.2 mm.

The hemi spherical dome of diameter 100 mm has been made by RAISHF by using software-based tool path planning for comparison of the two processes. The actual shapes produced by both the processes are shown in Fig. 4.16 (b) and (c). The dome height and force at the breakage have recorded by the equipped force measuring device and are presented in Table 4.7. The dome height obtained by RAISHF was 48.91 mm; thus, a rise of 190.2% has been observed by RAISHF, with respect to the conventional biaxial stretching. The nature of localized deformation coupled with pressure-induced ductility could be the possible reasons behind the enhancement of deformation by RAISHF process to such an extent.

Table 4.7: Comparison of RAISHF with biaxial stretching.

Material	Dome Height	Force at breakage
RAISHF	16.20 mm	4.19 kN
LDH	48.91 mm	1.86 kN

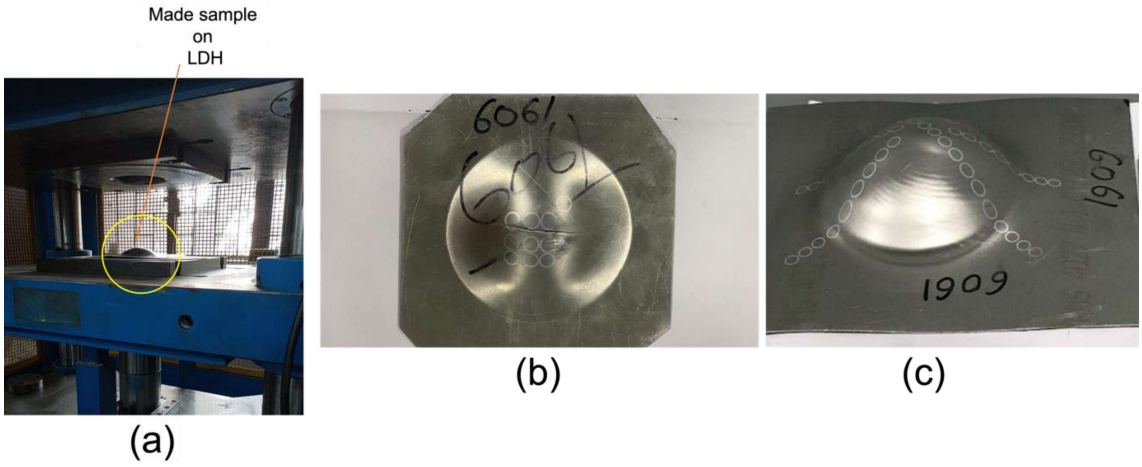

Figure 4.16: (a) Sample on hydraulic press, (b) Spherical dome produced during LDH test, and (c) Spherical dome produced by RAISHF.

Once similar domes had been formed by both the processes, FLC was made for the both and is demonstrated in Figure 4.17. For making FLC gridding method has been adopted, as explained earlier. Expectedly, in the case of LDH test using a hydraulic punch, scatter points lied very near to y = x line, suggesting that the mode of deformation is bi-axial stretching. The points obtained for RAISHF were well above those of LDH. Safe strain region in case of RAISHF is found to be significantly more than that in conventional forming.

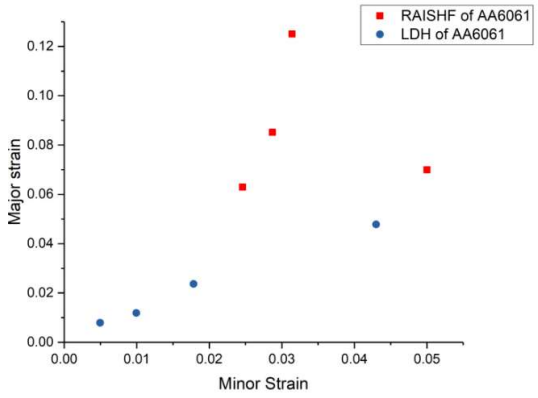

Figure 4.17: Forming limit diagram for the samples obtained from LDH test and RAISHF for the Al alloy 6061.

4.5 Conclusions

In this Chapter, a comparative study of forming of the AA 6061 sheet by two forming processes, RAISF and RAISHF, has been presented. Tensile test and Erichsen ductility test have been performed to evaluate tensile properties and formability of the sheet before deformation. Several shapes have been made using the two processes and their properties have been compared. Experiments have been performed on parameters obtained from straight groove test and the following conclusions are drawn.

- An increase of 6.67 % and 28.47% in maximum formable wall angle and forming depth has been observed by the RAISHF process. Additionally, spring back reduced by 77.14% in case of RAISHF in respect of RAISF.
- Due to hydrostatic nature of fluid pressure from back, more uniform thickness distribution is observed in case of RAISHF than that of RAISF. The average sheet thickness of the cone formed by RAISHF is 12.09% more than that formed by RAISF. It is further observed that the range of deviation of thickness values from average value varied from -9.87% to 17.27% in case of RAISF; whereas in case of RAISHF the variation lied in the range of -7% to 5%.
- Uniaxial tensile test has been conducted on the samples taken from the sheets before and after deformation. It has been revealed from the tensile test that strength of the formed cone is found to be higher due to strain hardening. Strength of the cone formed by RAISHF is found to be marginally higher than that formed by RAISF. Ductility is found to be more in samples formed by RAISHF due to pressure-induced ductility.
- Measurement of R_a revealed that finish of the surface in contact of tool is found to be better from RAISHF than from RAISF. An increase of 10.56% was observed in

the surface finish of the formed cone by RAISHF than by RAISF. AFM images revealed that surface topology of hydroformed sample is more uniform in comparison with incrementally formed samples. Hence, static fluid pressure from back can improve the surface quality of the formed product.

- It has been revealed from FLC of RAISHF and RAISF that FLD for RAISHF is found to be raised due to larger formability of sheet in that process. More in-plane strain was obtained in case of RAISHF than in RAISF.
- Finally, the micro hardness of the samples has been measured and is found that the sample in the middle region is hardest for both the alloys 6061. Microhardness in case of RAISF is found to be higher than that in RAISHF.
- XRD analysis has been carried out to find out the residual stresses in the samples taken from undeformed and formed samples by RAISF and RAISHF. More residual tensile stress has been observed in case of RAISF. The residual stress in both the cases was tensile in nature.
- EBSD analysis has been carried out for studying the microstructural evolution in the undeformed and formed by RAISF & RAISHF. It has been observed that significant grain refinement occurred from RAISF and RAISHF. Finer grains are found to be present in case of RAISF than in RAISHF. High density LAGBs were present in case of both RAISF and RAISHF samples. Majority of LAGBs in case of RASIF belonged to the group of 5^0-15^0 and in case of RAISHF majority of LAGBs belonged to the group of 2^0-5^0.
- It can be seen from the above points that RAISHF is a better process of sheet metal forming than RAISF in respect of process capabilities to form axis symmetric shapes. As ISF offers higher formability than conventional bi-stretching, hence

Limiting Dome Height test has been conducted in which hemispherical dome has been made on a hydraulic press and by RAISHF respectively. The measurements of dome height revealed that there was a rise of 186% in height of the domes. This rise is because of the nature of localized deformation and propagation of the same to a new location which leads to either suppression or delay of necking.

This chapter established RAISHF as a more capable process than that of RAISF. To further improve the process capabilities of RAISHF, multi-stage RAISHF can be adopted. The multi stage ISF has been reported to have improved the surface qualities of the formed product. The multi stage RAISHF performed on the existed setup and its comparative analysis with respect to single stage RAISHF has been discussed in the next chapter.